

Acta Mech  
DOI 10.1007/s00707-010-0376-8

---

Mario Di Paola · Antonina Pirrotta · Roberta Santoro

# De Saint-Venant flexure-torsion problem handled by Line Element-less Method (LEM)

Received: 10 May 2010  
© Springer-Verlag 2010

**Abstract** In this paper, the De Saint-Venant flexure-torsion problem is developed via a technique by means of a novel complex potential function analytic in all the domain whose real and imaginary parts are related to the shear stresses. The latter feature makes the complex analysis enforceable for the shear problem. Taking full advantage of the double-ended Laurent series involving harmonic polynomials, a novel element-free weak form procedure, labelled Line Element-less Method (LEM), is introduced, imposing that the square of the net flux across the border is minimized with respect to expansion coefficients. Numerical implementation of the LEM results in systems of linear algebraic equations involving positive-definite and symmetric matrices solving only contour integrals. Some numerical applications are reported to assess not only the efficiency and accuracy of the method to handle shear stress problems but also the robustness in the sense that exact solutions when available are captured straight away.

## 1 Introduction

The evaluation of shear stresses due to torsion and shear forces applied on a De Saint-Venant cylinder is a well-established problem in classical strength of material. However, because of mathematical difficulties that are inherent in the problem, only few analytical solutions have been developed for beams and shafts and the evaluation of the shear stress field is obtained via Finite Element Method (FEM) [1] and Boundary Element Methods (BEM) in symmetric [2–6] and non-symmetric form (see e.g. Katsikadelis [7] and references cited herein), which are both powerful methods for the analysis of structural systems. In more detail, FEM has been used for the solution of the two-dimensional torsion problem [8,9] for arbitrary cross-sections. Solutions obtained via FEM of simple and immediate use are affected, for accuracy sake, of a large number of elements in case of complicated cross-sections. Moreover, the FEM-based approach is also limited with respect to the shape of the elements yielding cumbersome meshing processes. On the other hand, the BEM integral method requires only discretization of the boundary, resulting in line elements as proposed for the torsion problem [10] of the De Saint-Venant beam. Analysis of the shear stress field in the presence of torsion and shear forces has

---

M. D. Paola · A. Pirrotta (✉) · R. Santoro  
Dipartimento di Ingegneria Strutturale, Aerospaziale e Geotecnica (DISAG),  
Università degli Studi di Palermo, Viale delle Scienze, 90128 Palermo, Italy  
E-mail: antonina.pirrotta@unipa.it  
Tel.: +39-091-6568424  
Fax: +39-091-6568407

M. D. Paola  
E-mail: mario.dipaola@unipa.it

R. Santoro  
E-mail: roberta.santoro@unipa.it

been proposed by Lacarbonara and Paolone [11] and via the BEM approach by Friedman and Kosmatka [12] and more recently, for anisotropic De Saint Venant cylinders, by Gaspari and Aristodemo [13]. The solution of the De Saint-Venant problem for shear and torsion obtained via FEM and BEM has also been used to evaluate shear and torsion factors in three-dimensional beam elements [14]. Furthermore, it is well known how useful complex analysis can be for studying the torsion problem [15, 16] using a classical potential function composed of a warping function and its harmonic conjugate function. Framed into this, in a recent paper [17] the authors propose to solve the problem of pure torsion in the De Saint-Venant cylinder by using a novel method labelled Line Element-less Method (LEM). Since the complex potential function is holomorphic in the whole domain, the proposed method takes full advantage of the double-ended Laurent series involving harmonic polynomials, which are fully capable to represent any analytic function in a complex domain. The selected expression of this analytic complex function is such that governing equations of De Saint-Venant elastic problem are satisfied in the cross-section domain but it does not satisfy the condition of vanishing net flux of the shear stress field across the border. This latter condition has been satisfied imposing in a weak form that the square value of the net flux across the border is minimized with respect to parameter expansions. Numerical implementation of the LEM results in systems of linear algebraic equations in positive-definite and symmetric matrices solving only contour integrals. Since the method does not require any meshing procedure but only requires integrations on a contour (element-less), it has been properly labelled *Line Element-less Method* (LEM). In [18], the authors show how competitive the LEM is in comparison with the complex polynomial method (CPM) [19] and the complex variable boundary method (CVBEM) [16]. Especially regarding the robustness of the method, it is capable to capture exact solutions (when available) only retaining a few series coefficients and exactly satisfying the boundary condition continuously.

It has to be remarked that so far no advantage of complex analysis is available in literature (to the authors best knowledge) for solving shear problems.

In this paper, the LEM is extended to the case of flexure and torsion by introducing a novel potential function related to shear stress straightaway. Some numerical applications to simply and multiply-connected domains have been reported to demonstrate the accuracy and the efficiency of the proposed method to handle shear stress problems. The method is robust in the sense that for all sections whose solution is known in analytic form (circular, elliptical and equilateral triangular with  $\nu = 0.5$ ) it provides the shear stress distribution exactly.

## 2 Theoretical background

In this section some well-known concepts of the classical theory of flexure are presented for sake of clarity as well as for introducing appropriate symbols. For further details, see Ziegler [20], Timoshenko [21], Timoshenko and Goodier [22], and Muskhelishvili [15].

Let us consider a linearly elastic and isotropic De Saint-Venant cylinder of length  $L$  and cross-section  $A$  with contour  $C$ . The cylinder is referred to a counter-clockwise coordinate system with  $x$ - and  $y$ -axes coincident, as customary, with the principal axes of inertia of the cross-section as shown in Fig. 1.

Let us assume that external forces, applied at the cross-section  $z = L$ , have components  $T_x(L)$ ,  $T_y(L)$  and  $M_z(L)$ , respectively (see Fig. 1). The stress field in the De Saint-Venant cylinder is completely defined by normal stress  $\sigma_z(z)$  and shear stresses  $\tau_{zx}(x, y)$ ,  $\tau_{zy}(x, y)$ . The normal stress  $\sigma_z(z)$  depends on shear induced bending moments  $M_x(z)$  and  $M_y(z)$ :

$$\sigma_z(z) = M_x(z)y/I_x - M_y(z)x/I_y, \quad (1)$$

$I_x$  and  $I_y$  being inertia moments of the cross-section with respect to the  $x$ - and  $y$ -axes, respectively. The shear stress fields  $\tau_{zx}(x, y)$  and  $\tau_{zy}(x, y)$  may be obtained by solving the equilibrium equation of the De Saint-Venant cylinder:

$$\partial\tau_{zx}/\partial x + \partial\tau_{zy}/\partial y = \operatorname{div}\boldsymbol{\tau} = -\partial\sigma_z/\partial z \quad \text{in } A, \quad (2)$$

with  $\boldsymbol{\tau}^T = [\tau_{zx} \ \tau_{zy}]$ , in conjunction with the compatibility conditions expressed by the two Beltrami equations for  $\tau_{zx}(x, y)$  and  $\tau_{zy}(x, y)$  expressed as:

$$\nabla^2\tau_{zx} + \frac{1}{1+\nu}\frac{\partial^2 I_1}{\partial x\partial z} = 0; \quad \nabla^2\tau_{zy} + \frac{1}{1+\nu}\frac{\partial^2 I_1}{\partial y\partial z} = 0 \quad \text{in } A, \quad (3a, b)$$

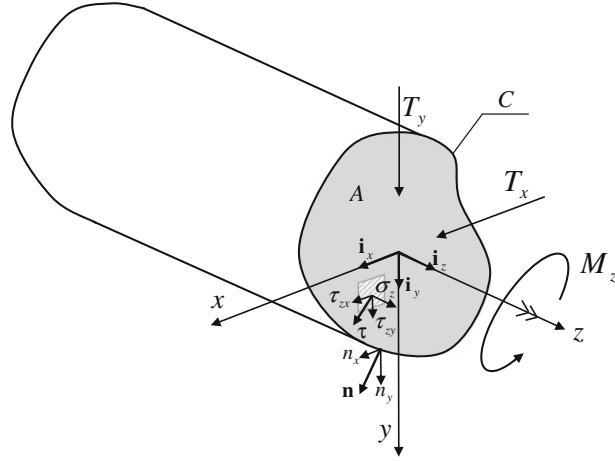


**Fig. 1** De Saint Venant cylinder under flexure-torsion

where  $\nabla^2 [\bullet] = \partial^2[\bullet]/\partial x^2 + \partial^2[\bullet]/\partial y^2$  and  $I_1 = \sigma_x + \sigma_y + \sigma_z = \sigma_z$  is the first invariant of the stress tensor;  $\nu$  is the Poisson ratio.

The boundary condition associated with the shear stresses is

$$\tau_{zx}n_x + \tau_{zy}n_y = \boldsymbol{\tau}^T \mathbf{n} = 0 \quad \text{on } C, \quad (4)$$

where  $C$  is the contour of the cross-section and  $\mathbf{n}^T = [n_x \ n_y]$  is a vector collecting the components of the outward normal to the contour  $C$ . Substitution of Eq. (1) expressing the normal stress  $\sigma_z$  into Eqs. (2, 3a, b) yields the governing equations for the shear stresses  $\tau_{zx}(x, y)$  and  $\tau_{zy}(x, y)$  as

$$\text{div } \boldsymbol{\tau} = -\frac{T_y}{I_x}y - \frac{T_x}{I_y}x \quad \text{in } A, \quad (5)$$

while the Beltrami equations in conjunction with Eq. (1) become

$$\nabla^2 \tau_{zx} = -\frac{1}{1+\nu} \frac{T_x}{I_y}; \quad \nabla^2 \tau_{zy} = -\frac{1}{1+\nu} \frac{T_y}{I_x} \quad \text{in } A, \quad (6a, b)$$

which may be also combined to yield the expression for  $\text{rot } \boldsymbol{\tau}$  of the shear stresses as

$$\frac{\partial \tau_{zy}}{\partial x} - \frac{\partial \tau_{zx}}{\partial y} = \mathbf{i}_z^T \text{rot } \boldsymbol{\tau} = \frac{\nu}{1+\nu} \left( \frac{T_y x}{I_x} - \frac{T_x y}{I_y} \right) + \text{const.} \quad \text{in } A, \quad (7)$$

where  $\mathbf{i}_z$  is the unitary vector along the  $z$  axis ( $\mathbf{i}_z^T = [0 \ 0 \ 1]$ ).

Moreover, the static equivalence conditions between shear stress field  $\boldsymbol{\tau}$  and shear forces  $T_x$  and  $T_y$  and torsion moment  $M_z$  on the cross-section domain are given respectively by

$$\int_A \tau_{zx} dA = T_x; \quad \int_A \tau_{zy} dA = T_y; \quad \int_A \boldsymbol{\tau}^T \mathbf{g} dA = M_z, \quad (8a, b, c)$$

where  $\mathbf{g}^T = [-y \ x]$ .

Summing up, the governing equations for the flexure-torsion problem consist in the equilibrium equation (2), in the compatibility conditions in Eq. (3a, b), with boundary condition expressed in Eq. (4) under the equivalence conditions expressed in Eqs. (8a, b, c).

### 3 Complex potential function formulation

Complex analysis in studying the torsion problem is an apparent tool as CPM [19], CVBEM [16] and LEM [18] assess. In the latter paper [18], a comparison of results obtained by properly approximating the classical potential function, according to the peculiarities of all three methods, is presented. This classical potential function is composed of the warping function and its conjugate harmonic function; moreover, in Di Paola et al. [17], the authors introduced LEM applied to a novel potential function related to shear stress straightaway and results coalesce with those obtained by applying LEM to the classical potential function [18]. Based on this solid ground, the idea of introducing this novel potential function makes it possible to take profit of complex analysis in studying shear and torsion problems as detailed in the following.

The elastic equilibrium problem for the De Saint-Venant cylinder may be efficiently formulated by complex analysis introducing an analytic function  $F(\hat{z})$  in the cross-section domain. The complex variable  $\hat{z} = x + iy$  (being  $i$  the imaginary unit) is defined in  $A$  and the function  $F(\hat{z})$  may be considered, in algebraic form, by the sum of real and imaginary components:

$$F(\hat{z}) = \chi_x(x, y) + i\chi_y(x, y). \quad (9)$$

The analytic requirement of the complex function  $F(\hat{z})$  is fulfilled under the restrictions that  $\chi_x(x, y)$  and  $\chi_y(x, y)$  are harmonic real functions so that they satisfy the conditions

$$\nabla^2 \chi_x = 0; \quad \nabla^2 \chi_y = 0 \quad \text{in } A \quad (10a, b)$$

and  $\chi_y$  is the conjugate harmonic of the function  $\chi_x$  so that they fulfil Cauchy-Riemann conditions, namely:

$$\partial \chi_x / \partial x = \partial \chi_y / \partial y; \quad \partial \chi_x / \partial y = -\partial \chi_y / \partial x \quad \text{in } A. \quad (11a, b)$$

As mentioned before, a novel formulation for the shear solution is introduced in this paper assuming that the real and the imaginary components of the function  $F(\hat{z})$  are directly related to the shear stresses by the relations

$$\chi_x(x, y) = \tau_{zx}(x, y) + \frac{1}{1+\nu} \left( \frac{\nu T_y x y}{I_x} + \frac{T_x x^2}{2I_y} \right) + G\bar{\theta}y, \quad (12)$$

$$\chi_y(x, y) = -\tau_{zy}(x, y) - \frac{1}{1+\nu} \left( \frac{\nu T_x x y}{I_y} + \frac{T_y y^2}{2I_x} \right) + G\bar{\theta}x, \quad (13)$$

where  $G$  is the shear modulus of the material and  $\bar{\theta}$  is a still unknown constant. If  $T_x$  and  $T_y$  are zero and  $M_z$  is different from zero, then  $\bar{\theta}$  coincides with the unitary twist angle of the cross-section.

It is worth noting that the conditions expressed in Eq. (10a, b) by substitution of Eqs. (12, 13) lead to the Beltrami equations for the shear stresses  $\tau_{zx}$  and  $\tau_{zy}$  as reported in Eqs. (6a, b). This means that the stress distribution  $\tau$  fulfils equilibrium and compatibility equations in the cross-section  $A$  and then the field  $\tau$  takes also into account the tangential stress due to shear induced torsion when the centroid does not coincide with the shear centre.

Moreover, the Cauchy–Riemann conditions (11a, b) imply that the complex potential  $F(\hat{z})$  satisfies both equilibrium and compatibility conditions in the domain  $A$ .

For the case of pure torsion ( $T_x = T_y = 0$ ), the potential function described in Eqs. (12) and (13) coalesces with that already proposed in Di Paola et al. [17].

### 4 Line Element-less Method (LEM) for the shear problem

In this section, the method dubbed *Line Element-less Method* (LEM) will be proposed to handle beams under shear force. First, the case of bi-connected cross-sections will be investigated because other cases of simply and multiply-connected regions will be easier derived.

## 4.1 LEM in bi-connected cross-sections

Since the potential function  $F(\hat{z})$  in Eqs. (9, 12, 13) is analytic in all points belonging to the cross-section, it may be expanded in the double-ended Laurent series as

$$F(\hat{z}) = \sum_{\substack{k=-\infty \\ k \neq -1}}^{+\infty} \alpha_k (\hat{z} - \hat{z}_0)^k \quad \alpha_k, \hat{z}_0 \in \mathbb{C}. \quad (14)$$

In the Laurent expansion, the term corresponding to  $k = -1$  has to be excluded; the motivation for the exclusion of this term is reported in Appendix A.

In Eq. (14), the series  $\sum_{k=0}^{+\infty} \alpha_k (\hat{z} - \hat{z}_0)^k$  is called *regular part* and it is capable to express any analytic function in a given region and in its contour. The series  $\sum_{k=-\infty}^{-2} \alpha_k (\hat{z} - \hat{z}_0)^k$  is called *principal part* and accounts for singularities in  $\hat{z}_0$ . It follows that  $\hat{z}_0$  has to be selected inside the hollow. This happens because  $F(\hat{z})$  is analytic in the points belonging to the cross-section but we do not have information on possible singularities in the hollow. It will be shown that the principal part is essential for a correct stress evaluation in the bi-connected sections, but it must be disregarded for simply-connected cross-sections.

Powers  $\hat{z}^k$  will be denoted as  $P_k + iQ_k$  with  $P_k$  and  $Q_k$  the so-called *harmonic polynomials* ( $\nabla^2 P_k = 0$ ,  $\nabla^2 Q_k = 0 \forall k$ ). Recursive relationships to construct these polynomials and derivative rules will be reported in Appendix B.

By letting  $\alpha_k = a_k + ib_k$  ( $a_k, b_k \in \mathbb{R}$ ) in Eq. (14), the complex potential function may be expanded in terms of truncated harmonic polynomials as follows:

$$F(\hat{z}) = \chi_x(x, y) + i\chi_y(x, y) = \sum_{\substack{k=-r_1 \\ k \neq -1}}^{r_2} (a_k P_k - b_k Q_k) + i \sum_{\substack{k=-r_1 \\ k \neq -1}}^{r_2} (a_k Q_k + b_k P_k), \quad (15)$$

where  $r_1$  and  $r_2$  are the selected orders of truncation of the principal part and regular part of the Laurent series.

Equation (15) may be rewritten in compact form as

$$F(\hat{z}) = \mathbf{p}^T \mathbf{a} - \mathbf{q}^T \mathbf{b} + i(\mathbf{q}^T \mathbf{a} + \mathbf{p}^T \mathbf{b}), \quad (16)$$

where

$$\mathbf{p}(x, y) = \begin{bmatrix} P_{-r_1}(x, y) \\ \vdots \\ P_{-2}(x, y) \\ P_0(x, y) \\ \vdots \\ P_{r_2}(x, y) \end{bmatrix}; \quad \mathbf{q}(x, y) = \begin{bmatrix} Q_{-r_1}(x, y) \\ \vdots \\ Q_{-2}(x, y) \\ Q_0(x, y) \\ \vdots \\ Q_{r_2}(x, y) \end{bmatrix}; \quad \mathbf{a} = \begin{bmatrix} a_{-r_1} \\ \vdots \\ a_{-2} \\ a_0 \\ \vdots \\ a_{r_2} \end{bmatrix}; \quad \mathbf{b} = \begin{bmatrix} b_{-r_1} \\ \vdots \\ b_{-2} \\ b_0 \\ \vdots \\ b_{r_2} \end{bmatrix} \quad (17)$$

and hence from Eq. (12) and (13) the stress vector  $\boldsymbol{\tau}$  is written in the form

$$\boldsymbol{\tau}(x, y) = \mathbf{D}(x, y)\mathbf{w} - \mathbf{J}(x, y)\mathbf{t} + G\bar{\theta}\mathbf{g}, \quad (18)$$

where

$$\mathbf{D}(x, y) = \begin{bmatrix} \mathbf{p}^T & -\mathbf{q}^T \\ -\mathbf{q}^T & -\mathbf{p}^T \end{bmatrix}; \quad \mathbf{w} = \begin{bmatrix} \mathbf{a} \\ \mathbf{b} \end{bmatrix}; \quad \mathbf{J}(x, y) = \frac{1}{1+\nu} \begin{bmatrix} x^2/2I_y & \nu xy/I_x \\ \nu xy/I_y & y^2/2I_x \end{bmatrix}; \quad \mathbf{t} = \begin{bmatrix} T_x \\ T_y \end{bmatrix}. \quad (19a-d)$$

The stress distribution given in Eq. (18) fulfils equilibrium and compatibility equations in the cross-section domain  $A$ . However, since Eq. (18) constitutes a truncation of the Laurent series, the boundary condition expressed in Eq. (4) may not be fulfilled in each point of the contours.

The crucial point of the LEM consists in satisfying the boundary condition  $\boldsymbol{\tau}^T \mathbf{n} = 0$  on the external contour  $C_e$  and the internal one  $C_i$  in a weak form, that is the unknown coefficients  $\mathbf{w}$  will be selected in a such way

that the squared value net flux of the shear stress  $\boldsymbol{\tau}$  through the boundary of the domain is minimal under the equivalence condition, that is

$$\begin{cases} \mathfrak{S}(\mathbf{w}, \bar{\theta}) = \oint_C (\boldsymbol{\tau}^T \mathbf{n})^2 dC = \min_{\mathbf{w}, \bar{\theta}} & (20a) \\ \text{subjected to} & \\ \int_A \mathbf{R} \boldsymbol{\tau} dA = \mathbf{f} & (20b) \end{cases}$$

where

$$\mathbf{R}^T = \begin{vmatrix} 1 & 0 & -y \\ 0 & 1 & x \end{vmatrix}; \quad \mathbf{f}^T = |T_x \ T_y \ M_z| \quad (21)$$

and  $C$  is the union of external and internal contours.

By using the Lagrange multiplier method, the minimum problem in Eq. (20a) is transformed into the minimum of the enlarged functional

$$\mathfrak{S}(\mathbf{w}, \bar{\theta}, \boldsymbol{\lambda}) = \oint_C (\boldsymbol{\tau}^T \mathbf{n})^2 dC + \boldsymbol{\lambda}^T \left( \int_A \mathbf{R} \boldsymbol{\tau} dA - \mathbf{f} \right) = \min_{\mathbf{w}, \bar{\theta}, \boldsymbol{\lambda}}, \quad (22)$$

where  $\boldsymbol{\lambda}$  is the vector of Lagrange multipliers.

In order to maintain the pure line integral method, the integral extended to the cross-section in Eq. (22) has to be transformed into a line integral. This may be done by using Green's lemma and the properties of harmonic polynomials as it is shown in Appendix B.

By performing variations of the free enlarged functional, we get

$$\frac{\partial \tilde{\mathfrak{S}}}{\partial \mathbf{w}} = \mathbf{Q} \mathbf{w} - l + G \bar{\theta} \mathbf{s} + \lambda_1 \mathbf{c} + \lambda_2 \mathbf{d} + \lambda_3 \mathbf{h} = 0, \quad (23a)$$

$$\frac{\partial \tilde{\mathfrak{S}}}{\partial (G \bar{\theta})} = \mathbf{s}^T \mathbf{w} - V + G \bar{\theta} H + \lambda_3 I_p = 0, \quad (23b)$$

$$\frac{\partial \tilde{\mathfrak{S}}}{\partial \lambda_1} = \mathbf{c}^T \mathbf{w} - \frac{3 + 2\nu}{2(1 + \nu)} T_x = 0, \quad (23c)$$

$$\frac{\partial \tilde{\mathfrak{S}}}{\partial \lambda_2} = \mathbf{d}^T \mathbf{w} + \frac{3 + 2\nu}{2(1 + \nu)} T_y = 0, \quad (23d)$$

$$\frac{\partial \tilde{\mathfrak{S}}}{\partial \lambda_3} = \mathbf{h}^T \mathbf{w} + G \bar{\theta} I_p + \frac{1 - 2\nu}{2(1 + \nu)} \left( \frac{T_x}{I_y} I_{xyy} - \frac{T_y}{I_x} I_{yxx} \right) - M_z = 0, \quad (23e)$$

where

$$\begin{aligned} \mathbf{Q} &= 2 \oint_C \mathbf{D}^T \mathbf{nn}^T \mathbf{D} dC; \quad l = 2 \oint_C \mathbf{D}^T \mathbf{nn}^T \mathbf{J} t dC; \quad \mathbf{s} = 2 \oint_C \mathbf{D}^T \mathbf{nn}^T \mathbf{g} dC; \\ V &= 2 \oint_C \mathbf{t}^T \mathbf{J}^T \mathbf{nn}^T \mathbf{g} dC; \quad H = 2 \oint_C \mathbf{g}^T \mathbf{nn}^T \mathbf{g} dC. \end{aligned} \quad (24a-e)$$

Moreover,  $I_{xyy}$  and  $I_{yxx}$  are third-order inertia moments (see Appendix B) and the vectors  $\mathbf{c}$ ,  $\mathbf{d}$ ,  $\mathbf{h}$  are vectors whose evaluation involves only line integrals as it is shown in Appendix B.

Equations (23) constitute a set of  $4 + 2(r_1 + r_2)$  linear equations that may be easily solved providing  $\mathbf{w}$ ,  $\bar{\theta}$ ,  $\boldsymbol{\lambda}$  so that  $F(\hat{z})$  and  $\boldsymbol{\tau}$  may be evaluated according to Eqs. (16) and (18), respectively.

Important remarks are as follows:  $\mathbf{Q}$  is a symmetric and positive definite matrix; the point  $\hat{z}_0$  in the complex plane for the regular part may be selected as a different point in the principal part of the Laurent series, that is  $\hat{z}_0$  for the principal part must be selected into the hollow, but  $\hat{z}_0$  for the regular part of the Laurent series may be selected in any other point.

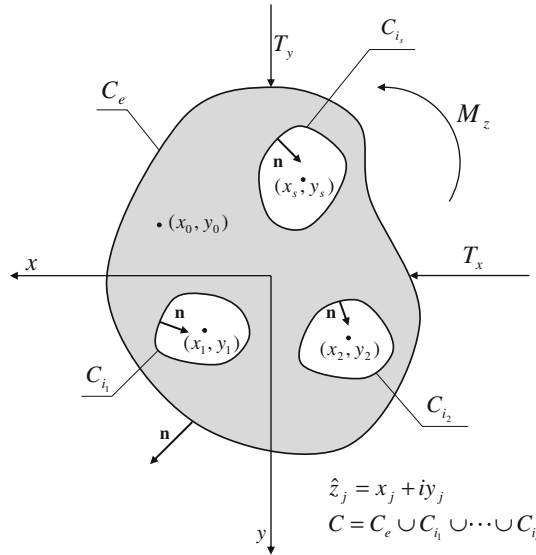


**Fig. 2** Multiply-connected cross-section and location of singularities  $\hat{z}_j$

#### 4.2 LEM in simply-connected cross-sections

The case of simply-connected cross-sections is obtained from the previous case simply by neglecting the principal part of the Laurent series, that is

$$F(\hat{z}) = \sum_{k=0}^{r_2} \alpha_k (\hat{z} - \hat{z}_0)^k = \sum_{k=0}^{r_2} (a_k P_k - b_k Q_k) + i \sum_{k=0}^{r_2} (a_k Q_k + b_k P_k), \quad (25)$$

that is all the equations remain the same but  $\mathbf{p}$ ,  $\mathbf{q}$ ,  $\mathbf{a}$ ,  $\mathbf{b}$  have to be defined in the form

$$\mathbf{p}(x, y) = \begin{bmatrix} P_0(x, y) \\ \vdots \\ P_{r_2}(x, y) \end{bmatrix}; \quad \mathbf{q}(x, y) = \begin{bmatrix} Q_0(x, y) \\ \vdots \\ Q_{r_2}(x, y) \end{bmatrix}; \quad \mathbf{a} = \begin{bmatrix} a_0 \\ \vdots \\ a_{r_2} \end{bmatrix}; \quad \mathbf{b} = \begin{bmatrix} b_0 \\ \vdots \\ b_{r_2} \end{bmatrix}. \quad (26)$$

The vectors  $\mathbf{c}$ ,  $\mathbf{d}$ ,  $\mathbf{h}$  (Appendix B) now contain  $r_2 + 1$  components and the solving system remains a linear system of  $6 + 2r_2$  equations in  $6 + 2r_2$  unknowns.

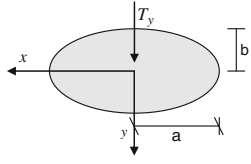
#### 4.3 LEM in multiply-connected cross-sections

As it has been stated in Sect. (4.1), the regular part of the Laurent series is totally independent of the principal part. Moreover, in multiply-connected domains we have polar singularities for each hollow, then we need the principal part of the Laurent series for each hollow, essential for the correct evaluation of the shear stress. That is, having  $s$  hollows in the cross-section, we have to select  $s$  points  $\hat{z}_j$  ( $j = 1, \dots, s$ ) inside the  $s$  hollows as it is shown in Fig. 2 and  $\hat{z}_0$  for the regular part is another point (that may be coincident with some  $\hat{z}_j$ ), and the function  $F(\hat{z})$  is then given as

$$F(\hat{z}) = \sum_{k=0}^{r_2} \alpha_k (\hat{z} - \hat{z}_0)^k + \sum_{j=1}^s \left( \sum_{k=-r_1}^{-2} \alpha_k^{(j)} (\hat{z} - \hat{z}_j)^k \right). \quad (27)$$

Then, all the concepts exploited in Sect. (4.1) do not change but  $\mathbf{D}(x, y)$ ,  $\mathbf{J}(x, y)$ ,  $\mathbf{g}$  have to be properly defined because new unknowns appear.

**Table 1** Results for shear stresses for an elliptical cross-section

Cross-section geometry	
Series coefficients $\neq 0$	$b_0 = -\frac{2(a^2+2b^2(1+\nu))T_y}{ab(a^2+3b^2)\pi(1+\nu)}$ ; $b_2 = \frac{2(1-2\nu)T_y}{ab(3a^2+b^2)\pi(1+\nu)}$
Lagrange multipliers $\bar{\theta}$	$\lambda = 0$ ; $\bar{\theta} = 0$
Shear stresses $\tau_{zx}(x, y)$	$-\frac{4[a^2\nu+b^2(1+\nu)]xyT_y}{ab^3(a^2+3b^2)\pi(1+\nu)}$
Shear stresses $\tau_{zy}(x, y)$	$\frac{2[2b^4(1+\nu)+b^2(a^2-2(1+\nu)y^2-(1-2\nu)x^2)-a^2y^2]T_y}{ab^3(a^2+3b^2)\pi(1+\nu)}$

## 5 Numerical studies

In this section, some applications on simply and multiply-connected cross-sections will be reported in order to show the effectiveness of the proposed method. It will also show the robustness of the LEM in the sense that it attains exact solution for all the cases in which it exists.

Exact solutions are marked since the stress field fulfills the boundary condition on  $C$ , in all the points of inner and outward contours. For all cases, a proper algorithm based on the theory described in the previous section has been developed using Mathematica 5.0. Shear centre and correction factors are evaluated by means of the expressions reported in Appendix C.

### 5.1 Simply-connected cross-sections

For a beam under shear forces exact solutions are known for elliptical and triangular cross-sections [22], the latter with  $\nu = 0.5$ . To assess the robustness of LEM both cases are studied considering only the regular part of the Laurent series expansion since both cross-sections (elliptical and triangular) are simply-connected.

In Tables 1 and 2 only the series coefficients  $a_k$ ,  $b_k$  different from zero are reported, no matter the value of truncation because all the others are exactly zero; the Lagrange multiplier  $\lambda$ , the value of  $\bar{\theta}$  and the  $\tau(x, y)$  function.

In particular, in Table 1, these values are provided for the ellipse under  $T_y$  and it is worth stressing that the expression of  $\tau(x, y)$  totally coincides with the exact solution reported in [22].

In Tables 2a, b, these values are reported for a triangular cross-section under  $T_x$  and  $T_y$ , respectively. All results are depending on  $\nu$ ; in the case of equilateral triangle the solution is exact and coincides with that reported in [22] for  $\nu = 0.5$ .

In Tables 3a, b, results are reported for isosceles triangular cross-section under  $T_x$  and  $T_y$ , respectively.

Opportune remarks have to be considered: for isosceles triangular cross-section with  $\nu = 0.5$  the solution obtained by LEM is exact since the condition  $\boldsymbol{\tau}^T \mathbf{n} = 0$  is fulfilled in all points of the boundary and for isosceles triangular cross-section with double height with respect to the base under shear force in  $y$ -direction, the solution is exact for every value of  $\nu$ .

### 5.2 Multiply-connected cross-sections

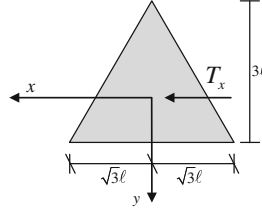
As it has been previously stated for the case of multiply-connected cross-sections, the principal part of the Laurent series is essential for each hollow in order to find a correct shear stress distribution for both shear forces and torsion moment.



**Table 2** Results for shear stresses for an equilateral triangular cross-section (a)  $x$ -direction shear force (b)  $y$ -direction shear force

(a)  $x$ -direction shear force

Cross-section geometry



Series coefficients  $\neq 0$   
Lagrange multipliers  $\bar{\theta}$

$$a_0 = \frac{2(41+32\nu)T_x}{171\sqrt{3}\ell^2(1+\nu)}; \quad a_2 = -\frac{(2\nu-1)T_x}{12\sqrt{3}\ell^4(1+\nu)}; \quad b_1 = -\frac{(45+62\nu)T_x}{228\sqrt{3}\ell^3(1+\nu)}$$

$$b_3 = \frac{35(2\nu-1)T_x}{1368\sqrt{3}\ell^5(1+\nu)}; \quad \lambda = 0; \quad \bar{\theta} = 0$$

Shear stresses  $(1 + \nu)\tau_{zx}(x, y)$

$$[16\ell^3(41 + 32\nu) + 6\ell^2(45 + 62\nu)y - 144\ell[y^2(1 - 2\nu) + x^2(3 + 2\nu)] + 35(3x^2 - y^2)(1 - 2\nu)y]T_x/1368\sqrt{3}\ell^5$$

Shear stresses  $(1 + \nu)\tau_{zy}(x, y)$

$$x[6\ell^2(45 + 62\nu) - 228\ell(1 + 2\nu)y + 35(x^2 - 3y^2)(1 - 2\nu)]T_x/1368\sqrt{3}\ell^5$$

Shear centre location

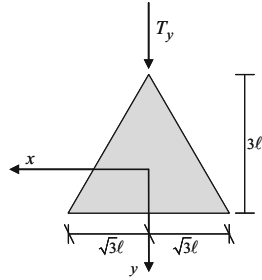
$$x_F = 0; \quad y_F = 0$$

Shear correction factor  $K_{XT}$

$$57(1 + \nu)/2(41 + 32\nu)$$

(b)  $y$ -direction shear force

Cross-section geometry



Series coefficients  $\neq 0$   
Lagrange multipliers  $\bar{\theta}$

$$a_1 = \frac{(45+62\nu)T_y}{228\sqrt{3}\ell^3(1+\nu)}; \quad a_3 = \frac{35(2\nu-1)T_y}{1368\sqrt{3}\ell^5(1+\nu)}; \quad b_0 = -\frac{2(41+32\nu)T_y}{171\sqrt{3}\ell^2(1+\nu)}$$

$$b_2 = -\frac{(2\nu-1)T_y}{12\sqrt{3}\ell^4(1+\nu)}; \quad \lambda = 0; \quad \bar{\theta} = 0$$

Shear stresses  $(1 + \nu)\tau_{zx}(x, y)$

$$x[6\ell^2(45 + 62\nu) - 228\ell(1 + 2\nu)y - 35(x^2 - 3y^2)(1 - 2\nu)]T_y/1368\sqrt{3}\ell^5$$

Shear stresses  $(1 + \nu)\tau_{zy}(x, y)$

$$[16\ell^3(41 + 32\nu) - 6\ell^2(45 + 62\nu)y - 114\ell[x^2(1 - 2\nu) + y^2(3 + 2\nu)] + 35(3x^2 - y^2)(1 - 2\nu)y]T_y/1368\sqrt{3}\ell^5$$

$\bar{\theta}$

$$0$$

Shear centre location

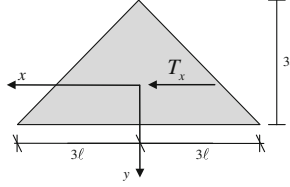
$$x_F = 0; \quad y_F = 0$$

Shear correction factor  $K_{YT}$

$$57(1 + \nu)/2(41 + 32\nu)$$

**Table 3** Results for shear stresses for an isosceles triangular cross-section (a)  $x$ -direction shear force (b)  $y$ -direction shear force(a)  $x$ -direction shear force

Cross-section geometry

Series coefficients  $\neq 0$   
Lagrange multipliers  $\bar{\theta}$ 

$$a_0 = \frac{(0.153+0.139\nu)T_x}{\ell^2(1+\nu)}; \quad a_2 = -\frac{0.012(2\nu-1)T_x}{\ell^4(1+\nu)}$$

$$b_1 = -\frac{(0.043+0.062\nu)T_x}{\ell^3(1+\nu)}; \quad b_3 = \frac{0.0009(2\nu-1)T_x}{\ell^5(1+\nu)}$$

$$\lambda_1 = -0.00013(1-2\nu)T_x/\ell^3(1+\nu); \quad \lambda_2 = 0$$

$$\lambda_3 = 0.00215(1-2\nu)T_x/\ell^4(1+\nu)$$

$$\bar{\theta} = -(0.0218 + 0.031\nu)T_x/\ell^3 G(1+\nu)$$

Shear stresses  $(1+\nu)\tau_{zx}(x, y)$ 

$$[\ell^3(0.153 + 0.139\nu) + \ell^2(0.065 + 0.092\nu)y - \ell[y^2(0.012 - 0.024\nu) + x^2(0.025 + 0.024\nu)] + (0.0027 - 0.0053\nu)x^2y - (0.001 - 0.002\nu)y^3]T_x/\ell^5$$

Shear stresses  $(1+\nu)\tau_{zy}(x, y)$ 

$$x[\ell^2(0.0215 + 0.03\nu) - \ell(0.024 + 0.026\nu)y + (0.001 - 0.002\nu)x^2 - (0.0027 - 0.0053\nu)y^2]T_x/\ell^5$$

Shear centre location

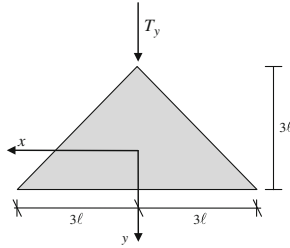
$$x_F = 0; \quad y_F = -(0.2 + 0.2811\nu)\ell/(1+\nu)$$

Shear correction factor  $K_{XT}$ 

$$84145.5(1+\nu)/(115737 + 105108\nu)$$

(b)  $y$ -direction shear force

Cross-section geometry

Series coefficients  $\neq 0$   
Lagrange multipliers  $\bar{\theta}$ 

$$a_1 = \frac{2T_y}{27\ell^3}; \quad a_3 = \frac{(2\nu-1)T_y}{162\ell^5(1+\nu)}; \quad b_0 = -\frac{2(7+4\nu)T_y}{81\ell^2(1+\nu)}; \quad b_2 = -\frac{(2\nu-1)T_y}{54\ell^4(1+\nu)}$$

$$\lambda = 0; \quad \bar{\theta} = 0$$

Shear stresses  $(1+\nu)\tau_{zx}(x, y)$ 

$$x[12\ell^2(1+\nu) - 6\ell(1+4\nu)y - (x^2 - 3y^2)(1-2\nu)]T_y/162\ell^5$$

Shear stresses  $(1+\nu)\tau_{zy}(x, y)$ 

$$(\ell - y)[4\ell^2(7+4\nu) + 4\ell(4+\nu)y - (3x^2 - y^2)(1-2\nu)]T_y/162\ell^5$$

Shear centre location

$$x_F = 0; \quad y_F = 0$$

Shear correction factor  $K_{YT}$ 

$$19\sqrt{3}(1+\nu)/2(41 + 32\nu)$$

For the annular cross-section depicted in Fig. 3a under shear force  $T_y$  the LEM (for  $\hat{x}_0 = 0$ ,  $\hat{y}_0 = 0$ ) returns only three coefficients of the Laurent expansion ( $b_{-2}$ ,  $b_0$  and  $b_2$ ) no matter the truncation orders  $r_1$  and  $r_2$ :

$$b_{-2} = -\frac{(3+2\nu)}{4(1+\nu)I_P} R_e^2 R_i^2 T_y; \quad b_0 = -\frac{(3+2\nu)}{4(1+\nu)I_P} (R_e^2 + R_i^2) T_y; \quad b_2 = \frac{(1-2\nu)}{4(1+\nu)I_P} T_y, \quad (28)$$

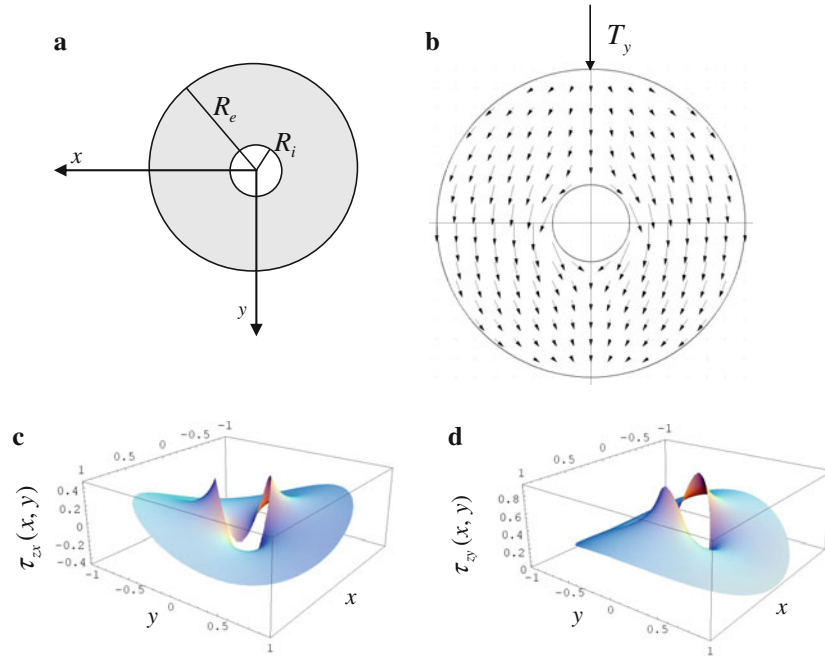


**Fig. 3** **a** Annular cross-section. **b** Shear stress field  $\tau$  due to a  $y$ -direction shear force in an annular cross-section ( $T_y = 1$ ,  $R_e = 1$ ,  $R_i = R_e/4$ ,  $\nu = 0.3$ ,  $r_1 = r_2 = 2$ ). **c** Shear stress function  $\tau_{zx}(x, y)$  in an annular cross-section subjected to a  $y$ -direction shear force ( $T_y = 1$ ,  $R_e = 1$ ,  $R_i = R_e/4$ ,  $\nu = 0.3$ ,  $r_1 = r_2 = 2$ ). **d** Shear stress function  $\tau_{zy}(x, y)$  in an annular cross-section subjected to a  $y$ -direction shear force ( $T_y = 1$ ,  $R_e = 1$ ,  $R_i = R_e/4$ ,  $\nu = 0.3$ ,  $r_1 = r_2 = 2$ )

where  $R_e$  and  $R_i$  are the external and internal radius, respectively and  $I_P = \pi(R_e^2 - R_i^2)/2$ . It has to be emphasized that this is an exact solution since  $\tau^T \mathbf{n} = 0$  proves to be locally fulfilled in the external and internal contour whatever the value of the Poisson ratio  $\nu$  is. A solution for the section under exam can be found in [23] in terms of *flexure function* expressed in polar coordinates. The presence of  $b_{-2}$  means that when the shear force is different from zero the solution has a polar singularity of order two. It is worth mentioning that from Eq. (28) if  $R_i = 0$  the polar singularity in zero disappears and if  $R_e = R$  coefficients of Eq. (28) are equal to those reported for elliptical cross-section setting  $a = b = R$  and  $T_x = M_z = 0$ .

Figures 3b–d show trajectories of  $\tau$  and shear stress functions  $\tau_{zx}(x, y)$  and  $\tau_{zy}(x, y)$  due to a  $y$ -direction shear force for the annular cross-section.

If the centre of the hollow does not coincide with the centre of the external contour (see Fig. 4a), then by selecting for the principal part  $\hat{z}_0$  in the centre of the hollow for  $T_x \neq 0$ ,  $T_y = 0$  (Fig. 4b) a solution is provided with  $b_k = 0 \forall k$  and  $a_k \neq 0 \forall k$ . In this case, the solution is not exact because the condition  $\tau^T \mathbf{n}$  is not locally fulfilled in all points of the contour. In particular, by selecting  $r_1 = r_2 = 3$  as truncation of the Laurent series the total flux  $\int_C (\tau^T \mathbf{n})^2 dC$  is negligible and the trajectories of the shear stress are depicted in Fig. 4b while c, d show the stress functions  $\tau_{zx}(x, y)$  and  $\tau_{zy}(x, y)$ . In presence of only  $T_y$  (Fig. 4e) LEM returns  $a_k = 0 \forall k$  and  $b_k \neq 0 \forall k$ . For this case, trajectories of the shear stress are depicted in Fig. 4e and in f, g the stress functions  $\tau_{zx}(x, y)$  and  $\tau_{zy}(x, y)$  are shown.

For the case of multiply-connected cross-section with two hollows (see Fig. 5a) as stressed in Sect. 4.3, we have to select  $\hat{z}_1$  and  $\hat{z}_2$  in the centres of the hollows while  $\hat{z}_0$  for the regular part has been selected for convenience in the origin of the axes. For the numerical application, the selected an outer radius  $R_e = 1$  and the two inner hollows radii are  $R_i^{(1)} = R_e/4$  and  $R_i^{(2)} = R_e/8$ , respectively.

Figures 5b–d show the shear stress trajectories and the shear stress functions  $\tau_{zx}(x, y)$  and  $\tau_{zy}(x, y)$  due to  $T_x$ , while in Figs. 5e, f, g the shear stress trajectories and the shear stress functions  $\tau_{zx}(x, y)$  and  $\tau_{zy}(x, y)$  due to  $T_y$  are depicted. It has to be remarked that for multiply-connected cross-sections, if we do not take into account for the principal part of Laurent expansion the shear stress distribution is totally wrong no matter the selected truncation order for the regular part of the Laurent expansion.

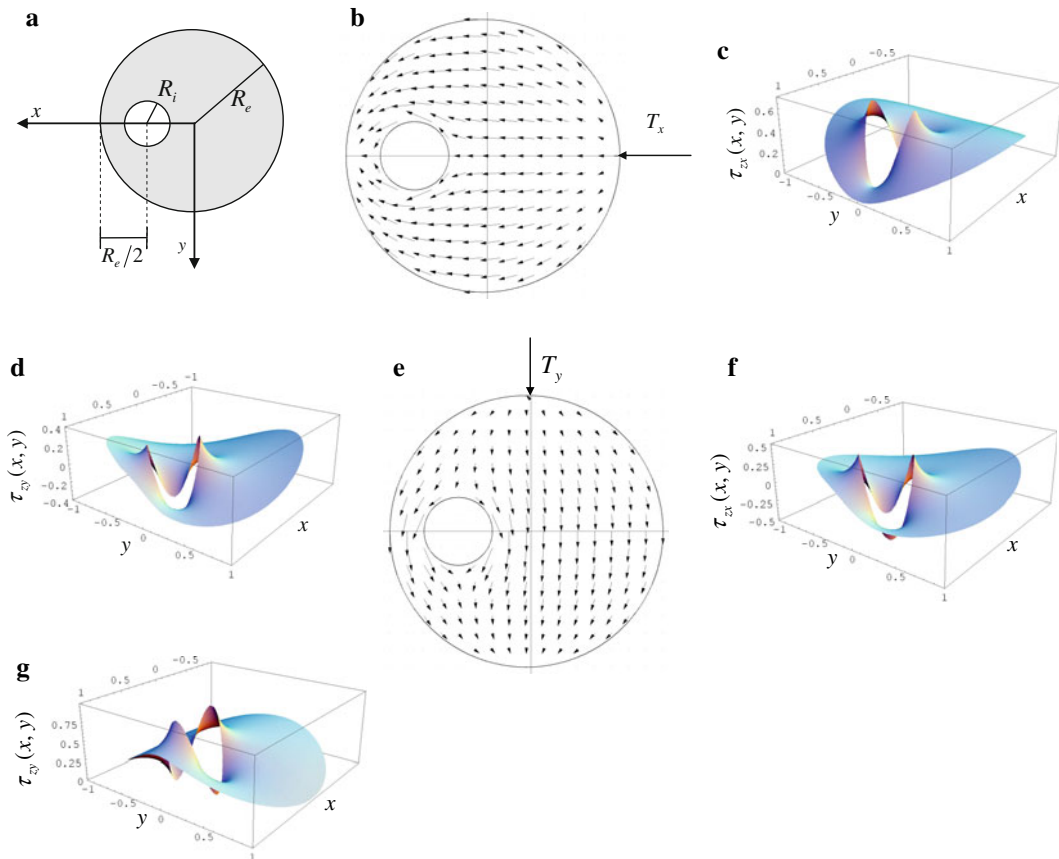


**Fig. 4** **a** Circular-hollow cross-section. **b** Shear stress field  $\tau$  due to an  $x$ -direction shear force in a circular-hollow cross-section ( $T_x = 1$ ,  $R_e = 1$ ,  $R_i = R_e/4$ ,  $\nu = 0.3$ ,  $r_1 = r_2 = 3$ ). **c** Shear stress function  $\tau_{zx}(x, y)$  in a circular-hollow cross-section subjected to an  $x$ -direction shear force ( $T_x = 1$ ,  $R_e = 1$ ,  $R_i = R_e/4$ ,  $\nu = 0.3$ ,  $r_1 = r_2 = 3$ ). **d** Shear stress function  $\tau_{zy}(x, y)$  in a circular-hollow cross-section subjected to an  $x$ -direction shear force ( $T_x = 1$ ,  $R_e = 1$ ,  $R_i = R_e/4$ ,  $\nu = 0.3$ ,  $r_1 = r_2 = 3$ ). **e** Shear stress field  $\tau$  due to a  $y$ -direction shear force in a circular-hollow cross-section ( $T_y = 1$ ,  $R_e = 1$ ,  $R_i = R_e/4$ ,  $\nu = 0.3$ ,  $r_1 = r_2 = 3$ ). **f** Shear stress function  $\tau_{zx}(x, y)$  in a circular-hollow cross-section subjected to a  $y$ -direction shear force ( $T_x = 1$ ,  $R_e = 1$ ,  $R_i = R_e/4$ ,  $\nu = 0.3$ ,  $r_1 = r_2 = 3$ ). **g** Shear stress function  $\tau_{zy}(x, y)$  in a circular-hollow cross-section subjected to a  $y$ -direction shear force ( $T_y = 1$ ,  $R_e = 1$ ,  $R_i = R_e/4$ ,  $\nu = 0.3$ ,  $r_1 = r_2 = 3$ )

## 6 Conclusions

The problem of stress distribution for the case of shear and torsion has been faced by *Line Element-less Method*. The method consists in defining a holomorphic function in the domain of the cross-section directly related to the shear stress distribution that will be expanded in the double-ended Laurent series. The potential function returns all the domain governing equations (equilibrium and compatibility) while the boundary condition ( $\tau^T \mathbf{n} = 0$ ) will be replaced in a weak form by properly minimizing the square net flux of the shear stress through the total contour (external and internal) under the static equivalence conditions. Use of Lagrange multiplier method gives the unknown coefficients of the Laurent series expansion. The solving equations involve a symmetric and positive definite matrix.

It is shown that for simply-connected regions the regular part of the Laurent expansion describes the solution in terms of stress. Vice-versa for multiply-connected regions some singularities happen in the hollows and then the principal part of the Laurent series is essential for description of the shear stress distribution.

The method is robust in the sense that for those regions where the shear stress distribution is already known, the LEM exactly reproduces such solutions. Moreover, some new exact shear stress distributions are obtained for cross-sections like isosceles triangular where the shear stress distribution fulfills the local condition on the contour continuously. For the other cases, the distribution is approximated and the more terms are inserted in the Laurent series expansion, the more accurate is the solution.

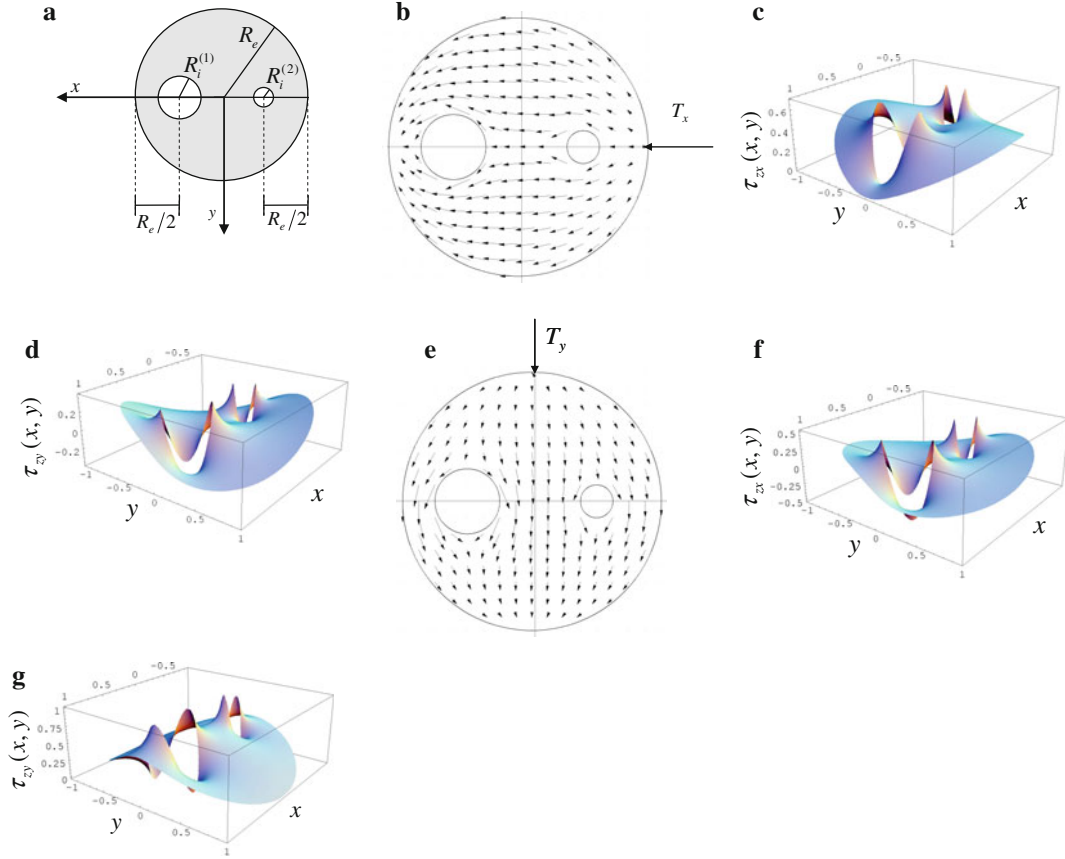


**Fig. 5** **a** Circular multiply-connected cross-section. **b** Shear stress field  $\tau$  due to an  $x$ -direction shear force in a circular multiply-connected cross-section ( $T_x = 1$ ,  $R_e = 1$ ,  $R_i^{(1)} = R_e/4$ ,  $R_i^{(2)} = R_e/8$ ,  $\nu = 0.3$ ,  $r_1 = r_2 = 3$ ). **c** Shear stress function  $\tau_{zx}(x, y)$  in a circular multiply-connected cross-section subjected to an  $x$ -direction shear force ( $T_x = 1$ ,  $R_e = 1$ ,  $R_i^{(1)} = R_e/4$ ,  $R_i^{(2)} = R_e/8$ ,  $\nu = 0.3$ ,  $r_1 = r_2 = 3$ ). **d** Shear stress function  $\tau_{zy}(x, y)$  in a circular multiply-connected cross-section subjected to an  $x$ -direction shear force ( $T_x = 1$ ,  $R_e = 1$ ,  $R_i^{(1)} = R_e/4$ ,  $R_i^{(2)} = R_e/8$ ,  $\nu = 0.3$ ,  $r_1 = r_2 = 3$ ). **e** Shear stress field  $\tau$  due to an  $y$ -direction shear force in a circular multiply-connected cross-section ( $T_y = 1$ ,  $R_e = 1$ ,  $R_i^{(1)} = R_e/4$ ,  $R_i^{(2)} = R_e/8$ ,  $\nu = 0.3$ ,  $r_1 = r_2 = 3$ ). **f** Shear stress function  $\tau_{xz}(x, y)$  in a circular multiply-connected cross-section subjected to an  $y$ -direction shear force ( $T_x = 1$ ,  $R_e = 1$ ,  $R_i^{(1)} = R_e/4$ ,  $R_i^{(2)} = R_e/8$ ,  $\nu = 0.3$ ,  $r_1 = r_2 = 3$ ). **g** Shear stress function  $\tau_{yz}(x, y)$  in a circular multiply-connected cross-section subjected to an  $y$ -direction shear force ( $T_x = 1$ ,  $R_e = 1$ ,  $R_i^{(1)} = R_e/4$ ,  $R_i^{(2)} = R_e/8$ ,  $\nu = 0.3$ ,  $r_1 = r_2 = 3$ )

### Appendix A: Motivation of exclusion of the term $k = -1$

Terms in the Laurent Series have a significant role depending on the physical meaning of the potential function at hand. For instance in [18] it has been stressed that in the Laurent series for solving torsion problems, since the classical potential function  $U(\hat{z})$  is related to the warping function  $\omega(x, y)$  and its harmonic conjugate  $\varphi(x, y)$  as

$$U(\hat{z}) = \omega(x, y) + i\varphi(x, y), \quad (\text{A1})$$

it is defined unless it is a constant, that means in the series we have to skip the term for  $k = 0$ .

On the other hand for solving torsion problems by the potential function  $F(\hat{z})$  related to shear stresses, we have to consider the term for  $k = 0$  in the Laurent series approximating  $F(\hat{z})$ , while in this case we have to skip the term for  $k = -1$  (in multi-connected domain). The latter condition arises from the relation between  $F(\hat{z})$  and  $U(\hat{z})$ :

$$\frac{dU(\hat{z})}{d\hat{z}} = F(\hat{z}). \quad (\text{A2})$$

Now let us suppose that only one hole is present in the cross-section (bi-connected cross-section), then  $U(\hat{z})$  may be approximated by the truncated double-ended Laurent expansion as follows:

$$U(\hat{z}) = \sum_{\substack{k=-r_1 \\ k \neq 0}}^{r_2} \beta_k (\hat{z} - \hat{z}_0)^k, \quad (\text{A3})$$

where, as customary,  $\hat{z}_0$  is selected into the hole of the cross-section.

It follows that, by setting  $\beta_k = m_k + in_k$  and taking into account Eq. (A3), the stress function  $\psi(x, y)$  may be written as

$$\psi(x, y) = G\theta \left[ \varphi(x, y) - \frac{1}{2}(x^2 + y^2) \right] \cong G\theta \left[ \sum_{\substack{k=-r_1 \\ k \neq 0}}^{r_2} (m_k Q_k + n_k P_k) - \frac{1}{2}(x^2 + y^2) \right] \quad (\text{A4})$$

and then the stresses  $\tau_{zx}(x, y)$  and  $\tau_{zy}(x, y)$ , taking into account the derivative rules of the harmonic polynomials exploited in Appendix B, may be expressed as

$$\begin{aligned} \tau_{zx}(x, y) &= \partial\psi(x, y)/\partial y \cong G\theta \sum_{\substack{k=-r_1 \\ k \neq 0}}^{r_2} (m_k k P_{k-1} - n_k k Q_{k-1}) - G\theta y, \\ \tau_{zy}(x, y) &= -\partial\psi(x, y)/\partial x \cong -G\theta \sum_{\substack{k=-r_1 \\ k \neq 0}}^{r_2} (m_k k Q_{k-1} + n_k k P_{k-1}) + G\theta x. \end{aligned} \quad (\text{A5a, b})$$

Examination of Eqs. (A5a, b) leads to conclude that  $\tau_{zx}$  and  $\tau_{zy}$ , obtained by expanding  $U(\hat{z})$  in the Laurent series (A3), do not contain the term  $1/(\hat{z} - \hat{z}_0)$ , corresponding to  $P_{-1}$  and  $Q_{-1}$ , since it is multiplied by zero. In other words, if we apply LEM to  $U(\hat{z})$  we get a solution in terms of  $\tau$  that does not contain  $P_{-1}$  and  $Q_{-1}$ . From these observations it is apparent that we do not have to integrate the terms  $P_{-1}$  and  $Q_{-1}$ , that is  $1/(\hat{z} - \hat{z}_0)$ , since this leads to a logarithmic term in the expressions of potential function or stress field, and consequently a multi-valued function.

As a conclusion in order to have a full consistency working either in terms of  $F(\hat{z})$  and  $U(\hat{z})$ , we may exclude the term involving  $1/(\hat{z} - \hat{z}_0)$  in the Laurent expansion of  $F(\hat{z})$  (Eq. 14) corresponding to  $k = -1$ .

Unfortunately, this correlation between terms of the series and physical meaning of the potential function has not been taken into account in [17] and then in the series expansion  $F(\hat{z})$  the term  $k = -1$  was erroneously retained. Thus, the Prandtl stress function and the warping function (Eqs. A1 and A2 in [17]) have to be rewritten as

$$\begin{aligned} \psi(x, y) &= G\theta \sum_{\substack{k=-r_1 \\ k \neq -1}}^{r_2} \left( a_k \frac{Q_{k+1}}{k+1} + b_k \frac{P_{k+1}}{k+1} \right) - \frac{G\theta}{2}(x^2 + y^2), \\ \omega(x, y) &= G\theta \sum_{\substack{k=-r_1 \\ k \neq -1}}^{r_2} \left( a_k \frac{P_{k+1}}{k+1} - b_k \frac{Q_{k+1}}{k+1} \right). \end{aligned} \quad (\text{A6a, b})$$

Obviously, if no hollows are present, then the aforementioned problem may be disregarded for both  $U(\hat{z})$  and  $F(\hat{z})$ . The problem for the coupled shear and torsion actions behaves in the same way.

In Fig. 6a is reported the same application as reported by Di Paola et al. [17] by using the series retaining the term for  $k = -1$  contrasted with the result in terms of stress function by using the correct expression (A6a) (without the term for  $k = -1$ ) (Fig. 6b).

From looking at the trajectories of the shear stress field (see Figs. 7a, b) especially in the closeness of the internal contour and between both contours, it is apparent that the correct solution is given by the series skipping the term for  $k = -1$  (Fig. 7b).

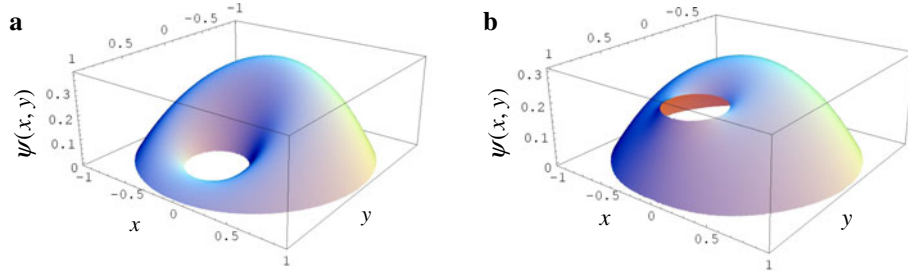


**Fig. 6** Prandtl stress function  $\psi(x, y)$  for pure torsion: **a**  $\psi(x, y)$  obtained retaining the term  $k = -1$  in the summation (incorrect); **b**  $\psi(x, y)$  obtained with Eq. A6a (correct)

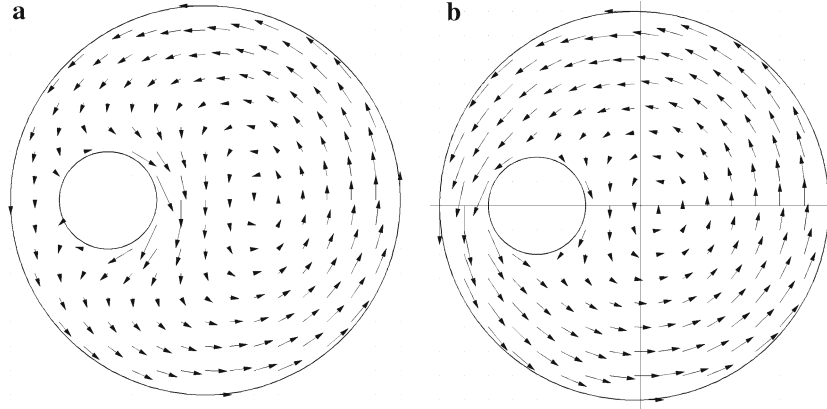


**Fig. 7** Stress trajectories for pure torsion: **a**  $\psi(x, y)$  obtained retaining the term  $k = -1$  in the summation (incorrect); **b**  $\psi(x, y)$  obtained with Eq. A6a (correct)

## Appendix B: Recursive form of harmonic polynomials and static equivalence condition

In this Appendix, the recursive forms of the harmonic polynomials  $P_k$  and  $Q_k$  are introduced together with their derivative property, in order to show how to rewrite the static equivalence condition involving a line integral only.

The harmonic polynomials  $P_k$  and  $Q_k$  are defined as follows:

$$P_k(x, y) = \operatorname{Re}[(x - x_0) + i(y - y_0)]^k; \quad Q_k(x, y) = \operatorname{Im}[(x - x_0) + i(y - y_0)]^k \quad (\text{B1})$$

and they may be evaluated recursively as

$$P_k(x, y) = P_{k-1}x - Q_{k-1}y; \quad Q_k(x, y) = Q_{k-1}x + P_{k-1}y \quad k > 0 \quad (\text{B2})$$

$$P_{-k}(x, y) = \frac{P_k(x, y)}{P_k^2(x, y) + Q_k^2(x, y)}; \quad Q_{-k}(x, y) = -\frac{Q_k(x, y)}{P_k^2(x, y) + Q_k^2(x, y)} \quad k > 0 \quad (\text{B3})$$

with  $P_0 = 1$ ,  $Q_0 = 0$ ,  $P_1 = x$ ,  $Q_1 = y$ .

The derivatives of the harmonic polynomials are

$$\frac{\partial P_k}{\partial x} = kP_{k-1}; \quad \frac{\partial P_k}{\partial y} = -kQ_{k-1}; \quad \frac{\partial Q_k}{\partial x} = kQ_{k-1}; \quad \frac{\partial Q_k}{\partial y} = kP_{k-1} \quad \forall k. \quad (\text{B4})$$

By taking full advantage of the relations ruling harmonic polynomial derivatives (Eq. B4), the static equivalence condition  $\int_A \mathbf{R}\tau dA = \mathbf{f}$  can be rewritten in the form

$$\sum_{\substack{k=-r_1 \\ k \neq -1}}^{r_2} a_k \int_A \operatorname{div} \mathbf{u}_k dA + \sum_{\substack{k=-r_1 \\ k \neq -1}}^{r_2} b_k \int_A \operatorname{div} \bar{\mathbf{u}}_k dA = \frac{3+2\nu}{2(1+\nu)} T_x, \quad (\text{B5a})$$

$$\sum_{\substack{k=-r_1 \\ k \neq -1}}^{r_2} a_k \int_A \operatorname{div} \mathbf{v}_k dA + \sum_{\substack{k=-r_1 \\ k \neq -1}}^{r_2} b_k \int_A \operatorname{div} \bar{\mathbf{v}}_k dA = -\frac{3+2\nu}{2(1+\nu)} T_y, \quad (\text{B5b})$$

$$\sum_{\substack{k=-r_1 \\ k \neq -1}}^{r_2} a_k \int_A \operatorname{div} \tilde{\mathbf{u}}_k dA + \sum_{\substack{k=-r_1 \\ k \neq -1}}^{r_2} b_k \int_A \operatorname{div} \tilde{\mathbf{v}}_k dA + G\bar{\theta} I_p + \frac{1-2\nu}{2(1+\nu)} \left( \frac{T_x}{I_y} I_{xyy} - \frac{T_y}{I_x} I_{yxx} \right) = M_z, \quad (\text{B5c})$$

where

$$\mathbf{u}_k = \frac{P_{k+1}}{k+1} \mathbf{i}_1; \quad \bar{\mathbf{u}}_k = \frac{P_{k+1}}{k+1} \mathbf{i}_2; \quad \mathbf{v}_k = \frac{Q_{k+1}}{k+1} \mathbf{i}_1; \quad \bar{\mathbf{v}}_k = \frac{Q_{k+1}}{k+1} \mathbf{i}_2; \quad \tilde{\mathbf{u}}_k = \frac{P_{k+1}}{k+1} \mathbf{g}; \quad \tilde{\mathbf{v}}_k = -\frac{Q_{k+1}}{k+1} \mathbf{g}. \quad (\text{B6})$$

In Eqs. (B6)  $\mathbf{i}_1$  and  $\mathbf{i}_2$  are given as

$$\mathbf{i}_1^T = [1 \ 0]; \quad \mathbf{i}_2^T = [0 \ 1] \quad (\text{B7})$$

and  $\mathbf{g}$  is defined in Eq. (8c).

Then, according to Green's lemma, Eq. (B5) may be rewritten as follows:

$$\mathbf{c}^T \mathbf{w} = \frac{3+2\nu}{2(1+\nu)} T_x; \quad \mathbf{d}^T \mathbf{w} = -\frac{3+2\nu}{2(1+\nu)} T_y; \quad \mathbf{h}^T \mathbf{w} + G\bar{\theta} I_p + \frac{1-2\nu}{2(1+\nu)} \left( \frac{T_x}{I_y} I_{xyy} - \frac{T_y}{I_x} I_{yxx} \right) = M_z \quad (\text{B8a-c})$$

with

$$\begin{aligned} \mathbf{c}^T &= |c_{-r_1} \dots c_{-2} c_0 \dots c_{r_2} \bar{c}_{-r_1} \dots \bar{c}_{-2} \bar{c}_0 \dots \bar{c}_{r_2}|, \\ \mathbf{d}^T &= |d_{-r_1} \dots d_{-2} d_0 \dots d_{r_2} \bar{d}_{-r_1} \dots \bar{d}_{-2} \bar{d}_0 \dots \bar{d}_{r_2}|, \\ \mathbf{h}^T &= |\tilde{c}_{-r_1} \dots \tilde{c}_{-2} \tilde{c}_0 \dots \tilde{c}_{r_2} \tilde{d}_{-r_1} \dots \tilde{d}_{-2} \tilde{d}_0 \dots \tilde{d}_{r_2}|, \end{aligned} \quad (\text{B9a-c})$$

where

$$\begin{aligned} c_k &= \oint_C \mathbf{u}_k^T \mathbf{n} dC; & \bar{c}_k &= \oint_C \bar{\mathbf{u}}_k^T \mathbf{n} dC; & d_k &= \oint_C \mathbf{v}_k^T \mathbf{n} dC; & \bar{d}_k &= \oint_C \bar{\mathbf{v}}_k^T \mathbf{n} dC; \\ \tilde{c}_k &= \oint_C \tilde{\mathbf{u}}_k^T \mathbf{n} dC; & \tilde{d}_k &= \oint_C \tilde{\mathbf{v}}_k^T \mathbf{n} dC \end{aligned} \quad (\text{B10})$$

and  $I_{xxy}$  and  $I_{yyx}$  are third-order moments of inertia as follows.

Geometrical properties of the cross-sectional area may be found developing line integral only. By using Green's lemma, we get

$$A = \int_A dA = \frac{1}{2} \oint_C (x n_x + y n_y) dC, \quad (\text{B11})$$

$$S_x = \int_A y dA = \frac{1}{2} \oint_C y^2 n_y dC; \quad S_y = \int_A x dA = \frac{1}{2} \oint_C x^2 n_x dC, \quad (\text{B12a, b})$$



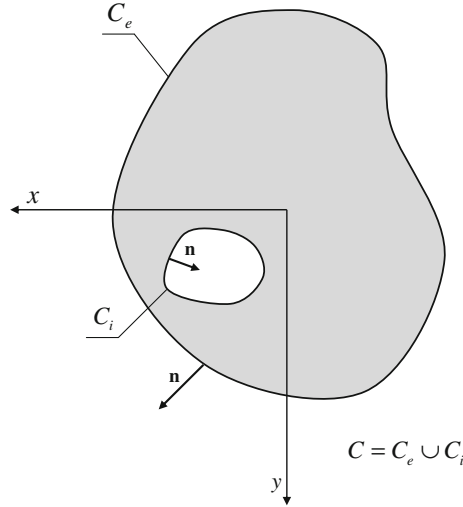


**Fig. 8** Outward normal to the cross-sectional area

$$I_x = \int_A y^2 dA = \frac{1}{3} \oint_C y^3 n_y dC; \quad I_y = \int_A x^2 dA = \frac{1}{3} \oint_C x^3 n_x dC, \quad (\text{B13a, b})$$

$$I_p = \int_A (x^2 + y^2) dA = \oint_C \left( \frac{x^3}{3} n_x + \frac{y^3}{3} n_y \right) dC; \quad I_{xy} = \int_A xy dA = \frac{1}{4} \oint_C xy (x n_x + y n_y) dC, \quad (\text{B14a, b})$$

$$I_{x_{yy}} = \int_A x^2 y dA = \oint_C (x^3 y/3) n_x dC; \quad I_{y_{xx}} = \int_A y^2 x dA = \oint_C (y^3 x/3) n_y dC, \quad (\text{B15a, b})$$

where  $C = C_e + C_i$  is the total contour (external and internal) and  $\mathbf{n}^T = [n_x \ n_y]$  is the outward normal to the cross-sectional area as shown in Fig. 8.

### Appendix C: Shear centre location and shear correction factor

As mentioned before, if  $T_x$  and  $T_y$  are zero and  $M_z$  is different from zero, then  $\bar{\theta}$  coincides with the unitary twist angle of the cross-section, while if  $M_z = 0$  and  $T_x$  and  $T_y$  are different from zero as well the centroid coincides with the shear centre  $F(x_F, y_F)$  it follows that  $\bar{\theta} = 0$ .

Based on these fundamental considerations, one can find the location of the shear centre following these steps:

- Setting  $T_x = T_y = 0, M_z = 1$  it follows from Eq. 18 a value of  $\bar{\theta}$  labelled as  $\bar{\theta}_1$
- Setting  $T_x \neq 0, T_y = M_z = 0$  it follows from Eq. 18  $\bar{\theta}$  say  $\bar{\theta}_x$  that is the unitary twist angle due to  $T_x y_F$ .
- Applying Betti's theorem to the two cases above considered it leads to  $T_x y_F \bar{\theta}_1 = \bar{\theta}_x$ .

Analogously, we can find the other coordinate, then it follows that:

$$x_F = \frac{\bar{\theta}_y}{\bar{\theta}_1 T_y}; \quad y_F = \frac{\bar{\theta}_x}{\bar{\theta}_1 T_x}. \quad (\text{C1a, b})$$

Once the location of the shear centre is known we can evaluate the stress field due to pure shear  $\boldsymbol{\tau}^S$  useful for the determination of shear correction factor, just considering the same problem as above (Eqs. 18, 20) in which  $\mathbf{f}$  is particularized as  $\mathbf{f}^T = [T_x \ T_y \ (-T_x y_F + T_y x_F)]$ .

Regarding the shear correction factor the formulation based on Timoshenko's definition (1940) is here reported. The shear correction factors in the  $x$  and  $y$ -direction, respectively, are expressed as:

$$K_{XT} = \frac{\int_A \tau_{zx}^S(x, y) dA}{A \tau_{zx}^S(x_G, y_G)}; \quad K_{YT} = \frac{\int_A \tau_{zy}^S(x, y) dA}{A \tau_{zy}^S(x_G, y_G)}, \quad (\text{C2a, b})$$

where in  $K_{XT}$ ,  $\tau_{zx}^S(x, y)$  is due to  $T_x \neq 0$  and  $T_y = 0$  and in  $K_{YT}$ ,  $\tau_{zy}^S(x, y)$  is due to  $T_y \neq 0$  and  $T_x = 0$ . The latter formulated in terms of harmonic polynomials are then rewritten as

$$K_{XT} = \frac{\left(\mathbf{c}^T \mathbf{w} - \frac{T_x}{2(1+\nu)}\right)}{A \tau_{zx}^S(x_G, y_G)}; \quad K_{YT} = -\frac{\left(\mathbf{d}^T \mathbf{w} + \frac{T_y}{2(1+\nu)}\right)}{A \tau_{zy}^S(x_G, y_G)}. \quad (\text{C3a, b})$$

The shear coefficients values depend only on the cross-sectional geometry and the Poisson ratio.

## References

1. Zienkiewicz, O.C.: The Finite Element Method in Engineering Science. McGraw-Hill, New York (1984)
2. Bonnet, M., Maier, G., Polizzotto, C.: Symmetric Galerkin boundary element method. *Appl. Mech. Rev.* **51**, 669–704 (1998)
3. Davì, G., Milazzo, A.: A symmetric and positive definite variational BEM for 2-D free vibration analysis. *Eng. Anal. Bound. Elem.* **14**, 343–348 (1994)
4. Davì, G., Milazzo, A.: A symmetric and positive definite BEM for 2-D forced vibrations. *J. Sound Vib.* **206**(4), 611–617 (1997)
5. Davì, G., Milazzo, A.: A new symmetric and positive definite boundary element formulation for lateral vibration of plates. *J. Sound Vib.* **206**(4), 507–521 (1997)
6. Panzeca, T., Cucco, F., Terravecchia, S.: Symmetric boundary element method versus finite element method. *Comput. Methods Appl. Mech. Eng.* **191**(31), 3347–3367 (2002)
7. Katsikadelis, J.T.: *Boundary Elements: Theory and Applications*. Elsevier Science Ltd, UK (2002)
8. Herrmann, R.L.: Elastic torsional analysis of irregular shapes. *ASCE J. Eng. Mech. Div.* **91**(EM6), 11–19 (1965)
9. Mason, W.E., Herrmann, R.L.: Elastic shear analysis of general prismatic shaped beams. *ASCE J. Eng. Mecha. Div.* **94**(EM4), 965–983 (1968)
10. Jawson, M.A., Ponter, A.R.: An integral equation solution of the torsion problem. *Proc. R. Soc. Lon.* **275**(A), 237–246 (1963)
11. Lacarbonara, W., Paolone, A.: On solution strategies to Saint–Venant problem. *J. Comput. Appl. Math.* **206**, 473–497 (2007)
12. Friedman, Z., Kosmatka, J.B.: Torsion and flexure of a prismatic isotropic beam using the boundary element method. *Comput. Struct.* **74**, 479–494 (2000)
13. Gaspari, D., Aristodemo, M.: Torsion and flexure analysis of orthotropic beams by a boundary element model. *Eng. Anal. Bound. Elem.* **29**, 850–858 (2005)
14. Petrolo, A.S., Casciaro, R.: 3D beam element based on Saint Venant's rod theory. *Comput. Struct.* **82**, 2471–2481 (2004)
15. Muskhelishvili, N.I.: *Some Basic Problems of the Mathematical Theory of Elasticity*. P. Noordhoff Ltd, Groningen, The Netherlands (1953)
16. Hromadka, T.V. II.: *The Complex Variable Boundary Element Method*. Springer, Berlin, Heidelberg, New York, Tokyo (1984)
17. Di Paola, M., Pirrotta, A., Santoro, R.: Line element-less method (LEM) for beam torsion solution (truly no-mesh method). *Acta Mech.* **195**(1–4), 349–364 (2008)
18. Barone, G., Pirrotta, A., Santoro, R.: Comparison among three boundary element methods for torsion problems: CPM, CVBEM, LEM. Submitted to *Engineering Analysis with Boundary Elements* (2010)
19. Poler, A.C., Bohannon, A.W., Schowalter, S.J., Hromadka, T.V. II.: Using the Complex Polynomial Method with Mathematica to Model Problems Involving the Laplace and Poisson Equations. Published online in Wiley InterScience ([www.interscience.wiley.com](http://www.interscience.wiley.com)) (2008). doi:10.1002/num.20365
20. Ziegler, F.: *Mechanics of Solid and Fluids*, 2nd reprint of 2nd edn. Springer, New York (1998)
21. Timoshenko, S.P.: *Strength of Materials-Part1*, 2nd edn. Van Nostrand, New York, NY (1940)
22. Timoshenko, S.P., Goodier, J.N.: *Theory of Elasticity*, 2nd edn. McGraw-Hill, New York, NY (1951)
23. Love, E.A.H.: *A Treatise on the Mathematical Theory of Elasticity*, 4th edn. Dover Publications, New York, NY (1926)